Chair of Urban Water Systems Engineering
TUM School of Engineering and Design
Technical University of Munich

Robust MPC of agricultural AD plant with uncertain substrate characterization

Prevention of constraint violation in a plant-model mismatch scenario

David Santiago M. Zarate

Study Project
Master of Science in Environmental Engineering
at TUM School of Engineering and Design of the Technical University of Munich

Examiner
Prof. Dr. Konrad Koch
Chair of Urban Water Systems Engineering

Supervised by
Simon Hellmann
Deutsches Biomasseforschungszentrum

Submitted by
David Santiago M. Zarate
Matriculation Number: 03772752

Submitted on
24.09.2024

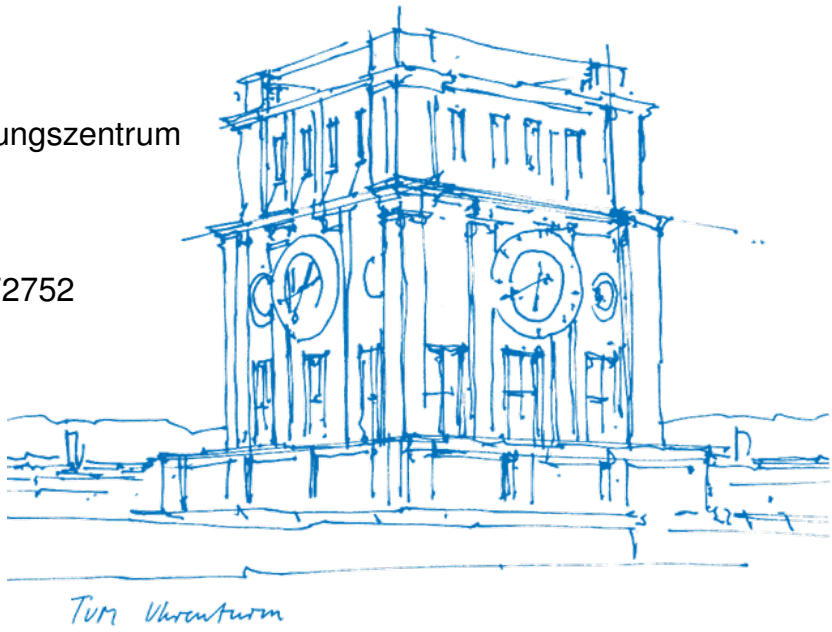

Abstract

Model Predictive Control (MPC) is recognized for its versatility in handling control of nonlinear systems under constraints. The model used in this study is the ADM1-R3-Core, a simplified version of the Anaerobic Digestion Model No. 1 (ADM1), commonly used for modeling of anaerobic digestion. In simulation studies, MPC requires models for both the controller and the plant. While these models can be identical, they typically differ in practice as no model is perfect. Due to this plant-model mismatch, it is essential to assess the robustness of the controller under such conditions, as constraint violations may arise.

This study compares the control performance of nominal and robust MPC controllers when a mismatch occurs in an agricultural biogas plant with uncertain substrate characterization. This research thereby contributes to developing model-based control of full-scale agricultural biogas plants.

Keywords: *MPC, substrate characterization, robust control, biogas, ADM1-R3, plant-model mismatch.*

Contents

List of Tables

List of Figures

1 Introduction

Demand-oriented biogas production from full-scale anaerobic digestion (AD) plants can help compensate for fluctuating electricity sources like wind and solar. Moreover, it might increase revenues for plant operators, who are increasingly challenged by state subsidy schemes gradually fading out. With the ADM1 reductions proposed by Weinrich and Nelles (2021), there exist powerful yet compact models to describe the AD process, suitable for application to agricultural biogas plants. A major source of model uncertainty originates from the substrate characterization, especially with regard to the fermentable macronutrients (carbohydrates, proteins, lipids).

This study is based on the previous work of Frontzek (2024) and investigates the control performance of model predictive control (MPC), explicitly taking into account these uncertainties. A special focus is laid on the robustness of the MPC controller in light of plant-model mismatch.

1.1 Modeling

1.1.1 ADM1-R3 model

The AD process was represented by the ADM1-R3-Frac in the thesis of Frontzek (2024), supervised by Simon Hellman, while in this work, the AD process was simulated using the ADM1-R3-Core. This model is a simplification of the ADM1 models proposed by Weinrich and Nelles (2021). It simulates the AD process as a two-step process, involving hydrolysis, acidogenesis and acetogenesis as the first step, and methanogenesis as the second; taking into account inhibition of the process through pH, ammonia, and nitrogen limitation. A scheme of the main model components of the ADM1-R3 is shown in Figure 1.

This model considers the mass concentration of the species as states, denoted by x_i; measurements, such as biogas volume flow and pH, denoted by y_i; and influent volume flow of individual agricultural substrates as control variables, denoted by u. Frontzek (2024) implemented a modified version named ADM1-R3-Frac, which divides carbohydrates into fast and slowly degradable for a better prediction of biogas production after feedings.

Other parameters for the modeling of AD processes are included. They are divided into time-invariant parameters, such as Henry constants, and time-varying parameters θ which are subject to calibration. Substrate characterization was considered uncertain; in

practice, carbohydrates are challenging to quantify as only the fermentable fraction is considered in the model for biogas production.

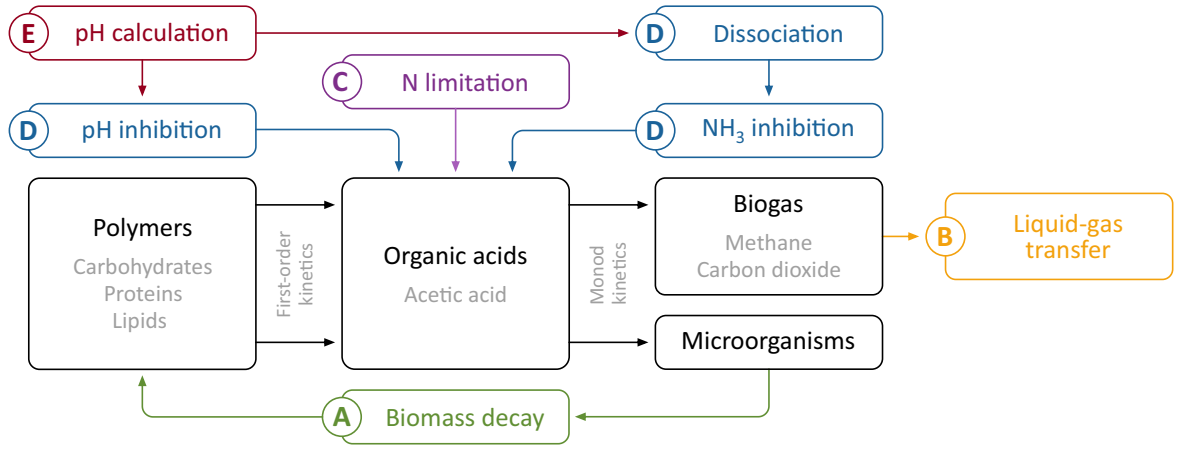

Figure 1. *A schematic illustration the model components of the ADM1-R3.*

1.1.2 ADM1-R3-Core model

The ADM1-R3-Core differs from the ADM1-R3 model by neglecting the water and ash states, as they are not relevant for assessing the process stability. Additional time-varying parameters were introduced to ensure proper calibration and fitting. To increase numerical robustness, this model was normalized by using arbitrary values for the states x, measurement y, and inputs u; the procedure is described in the Appendix.

1.2 Basics of MPC

1.2.1 MPC

MPC is a control strategy that uses a model to predict the future response of a system over a finite prediction horizon; Figure 2 illustrates state and control principles implemented in MPC schemes. MPC optimizes the input trajectory within this horizon by solving an optimization problem that minimizes an objective function, subject to constraints, based on the predicted system behavior. Once the optimal sequence of inputs is computed, only the first input of the sequence is applied to the plant. The plant state is then re-estimated and used as the initial value for the next optimization, with the prediction horizon shifted forward by one step.

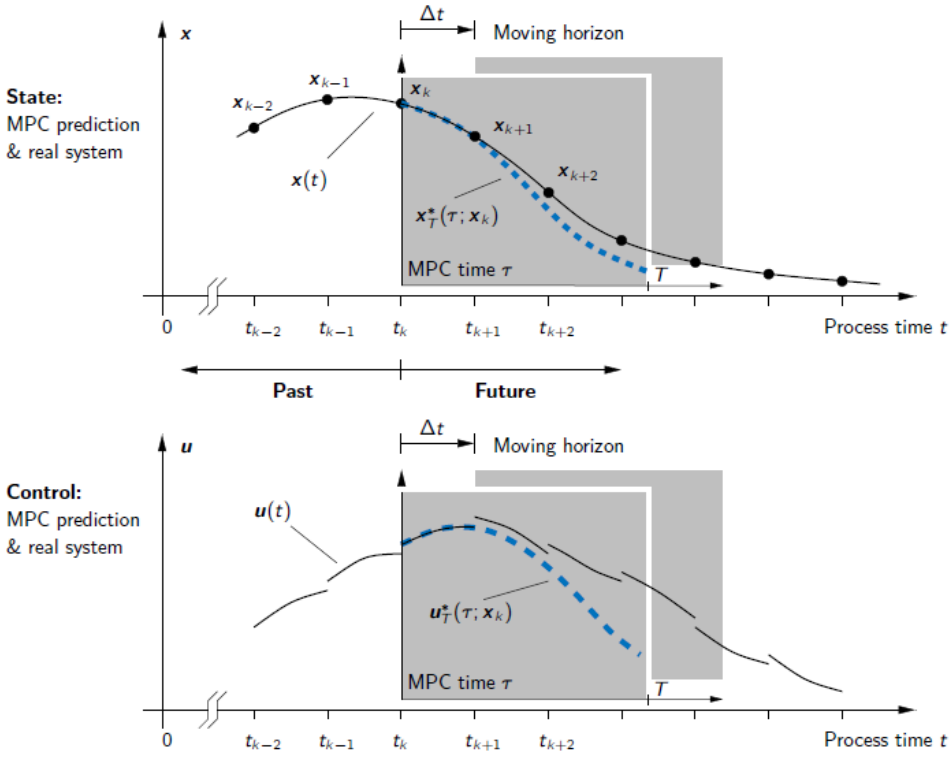

Figure 2. *State feedback on MPC when a plant-model mismatch is present. Taken from Graichen (2024)*

The MPC implementation is composed of three main blocks: the controller, simulator, and estimator. In a practical application, the simulator would be replaced by the real plant. The estimator receives measurements from the plant, replaced by the simulator in this work, and computes the optimal sequence inputs based on the predictions of the controller model. The simulator takes these inputs and computes the corresponding plant response. This response is then fed into the estimator, which estimates the plant state based on its measurements. These estimates are provided to the controller, which closes the control loop. A schematic representation of this process is shown in Figure 3.

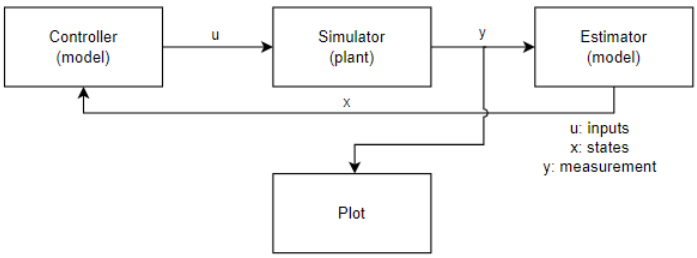

Figure 3. *Information flow in simulative MPC.*

1.2.2 Nominal and Robust MPC

One of the main advantages of MPC is that it allows the incorporation of robust control approaches to explicitly account for parametric plant-model mismatch. In the nominal case, the controller takes the nominal parameter value, which is used to calculate the system's output.

The multi-stage approach incorporates robustness into MPC, in which the controller is supplied with a set of possible values for the $uncertain$ parameters, generating a tree of different predicted scenarios. This scenario tree grows exponentially over time based on the number of uncertain variables and the range of values they can take. To maintain the tractability of this multi-scenario approach, a tuning parameter, known as the $robust\ horizon$ is introduced to limit the growth of the scenario tree. An example of a scenario tree for three different parameter values and a robust horizon of 2 is shown in Figure 4.

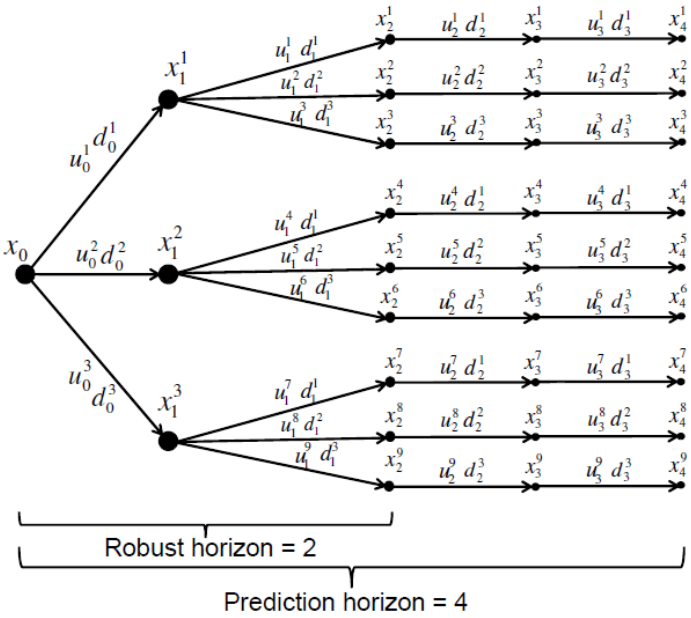

Figure 4. *Scenario tree on robust MPC with a robust horizon of 2, and a prediction horizon of 4. Taken from Lucia and Engell (2014)*

1.2.3 do-mpc toolbox

Fiedler et al. (2023) implemented an open-access MPC toolbox called do-mpc, which serves as the foundation for this work. This toolbox provides the necessary control, simulation, and estimation modules for simulating stiff nonlinear differential equation systems, such as the ADM1-R3.

The control problem involves minimizing an objective function subject to specified constraints. MPC constraint handling is one of its main advantages over other control approaches, as it allows the implementation of nonlinear constrained cost functions. The optimization process utilizes the package coin-or (Lougee, 2003), which acts as an interface between do-mpc and the optimization solver. During this phase, hard constraint violations may occur, rendering the simulation infeasible. Interior Point OPTimize (IPOPT) is a common library of solvers used by do-mpc and other MPC approaches to solve the underlying optimization problems. It addresses the issue of infeasibility through constraint violation by implementing a feasibility restoration phase, in which the problem enters an intermediate step aimed at reducing constraint violations and returning to a feasible state. Details on this algorithm can be found in Wächter and Biegler (2006).

2 Implementation

2.1 Migration from ADM1-R3-Frac to ADM1-R3-Core

ADM1-R3-Core is a simplified version of the ADM1-R3 model. This model includes 14 states with corresponding ordinary differential equations instead of 17. This is achieved by joining slow and fast fermentable carbohydrates into one state, omitting the individual states of water S_{h2o} and ashes X_{ash}, replacing the ion state S_{ion} with a time-variant parameter ΔS_{ion} for calibration of the pH, and introducing an additional parameter θ_9 to calibrate ammonium nitrogen. The equations are presented in the Appendix.

Frontzek (2024) computed the nominal values of carbohydrates x_{ch}, proteins x_{pr}, and lipids x_{li} based on BMP, total solids (TS), and TS-based concentration of ashes $\overline{X}_{ash}$. As ashes were removed as an individual state in the ADM1-R3-Core model, their concentration in the substrates was set to 0.

2.2 Analyzed scenarios

2.2.1 Methanation scenario

The methanation scenario simulates biogas production over a one-month period, during which set-point changes are applied over the first 9 days, followed by 21 days of steady-state operation. The primary objective of this scenario is to assess the tracking performance of a step-wise constant setpoint for methane production, specifically for a biogas upgrading methanation unit.

2.2.2 Cogeneration scenario

The cogeneration scenario simulates biogas production with flexible cogeneration over one month. This scenario incorporates a gas storage with a maximum volume of 385 m^3 and a minimum volume of 0 m^3, to buffer biogas consumption required according to a weekly schedule for the combined heat and power (CHP) plant. The primary objective is to ensure that the capacity limits of the biogas storage tank are not exceeded throughout the operation.

2.3 Treatment of X_{ash} and $S_{ion,in}$

In the ADM1-R3-Core model, the state S_{ion} is implemented as a constant parameter ΔS_{ion}. Based on the results obtained by Frontzek (2024) for the cogeneration scenario, a weighted average of the inlet concentrations of the individual substrates was calculated,

yielding a value of $\Delta S_{ion} = 0.0034 gL^{-1}$. Additionally, the tuning parameter θ_9 was set to 1. Comparative simulation results are presented in Figure 5.

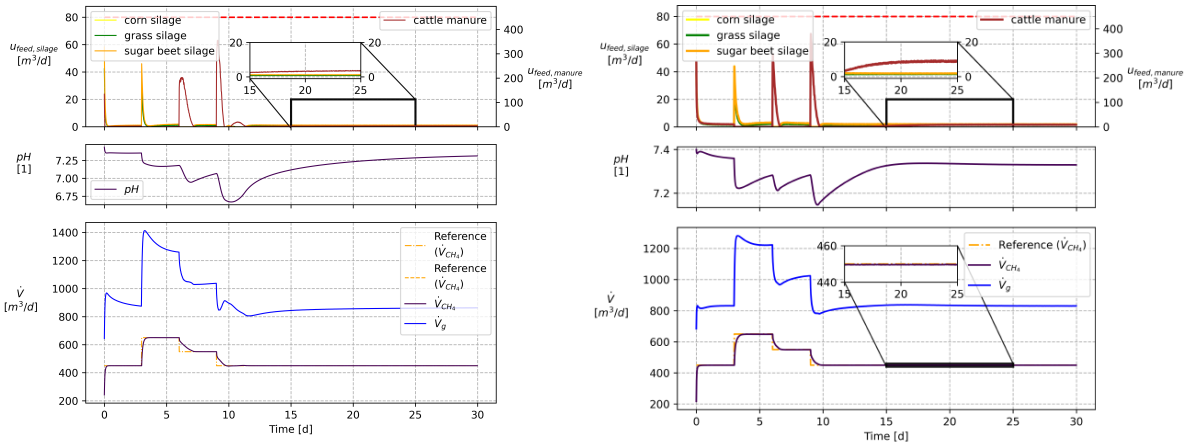

(a) *Result obtained with ADM1-R3-Core* ***(b)*** *Result obtained by Frontzek (2024)*

Figure 5. *Comparison of the results obtained for the methanation scenario by Frontzek (2024) and this work.*

2.4 Substrate uncertainties

For the methanation and cogenerations scenarios, the only source of uncertainty is the substrate inlet concentration. As a result, probability density curves were computed by Frontzek (2024) and are shown in Figure 6. The substrates chosen for these scenarios were corn silage, grass silage, cattle manure, and sugar beet silage.

2.5 Plant-Model mismatch

In this simulative study, the physical plant is replaced by a simulation. The underlying model of the plant differs from the controller model to account for plant-model mismatch. Specifically, a parametric plant-model mismatch is introduced for the inlet concentrations of carbohydrates, using standard deviations to represent the uncertainties, as these concentrations represent only the fermentable fraction of the total carbohydrates and are thus challenging to quantify accurately in real-world conditions.

2.5.1 State feedback scheme

In a real-world scenario, measurements from the plant are available, but the whole state of the plant is not known. In order for the MPC controller to make predictions, the value of the state of the plant at the start of each prediction horizon is required. To address this problem, MPC includes a state observer that gives the new initial state at each new

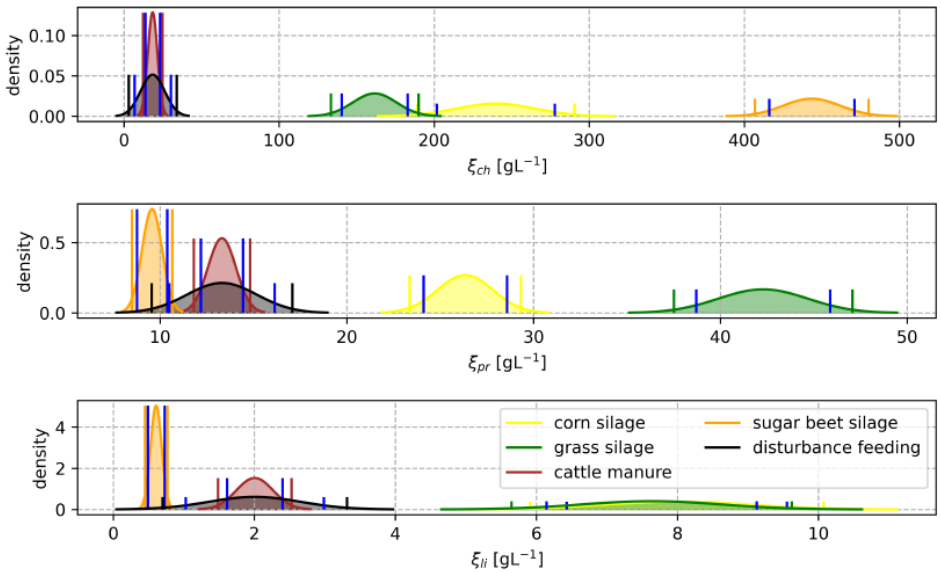

Figure 6. *Substrate density functions for carbohydrates, proteins, and lipids. Taken from Frontzek (2024).*

iteration. On a state feedback scheme, which is only valid in simulative scenarios, it is assumed that the state of the plant is known perfectly and this data is supplied back to the controller before the solution of each optimization problem.

As illustrated in Figure 2, predictions into the future are computed based on the *prediction horizon* for the next time steps. In case of a plant-model mismatch, the plant's state is provided as input to the controller, causing the predictions of the controller to differ from the realized results of the plant at each time step. This discrepancy is shown at the top of Figure 2, where the expected scenario is represented in the state graph, where the scenario expected by the controller is represented by the solid line and the realized value of the plant by the dashed blue line.

2.5.2 Sensitivity analysis

The ADM1-R3 model implemented by Frontzek (2024) considered influent carbohydrates, proteins, and lipids as uncertain variables; these uncertainties were calculated based on the observed uncertainty of the measurements for substrate characterization. It was assumed that uncertainties were independent, resulting in a linear uncertainty error propagation based on a reformulated standard deviation scheme. The resulting bounds were provided to the controller, while the bounds were calculated as a specified number of standard deviations above and below the nominal value. In contrast, the plant used a random value within these bounds in Frontzek (2024).

A sensitivity analysis was conducted to identify which macronutrient inlet concentration had the greatest influence on gas production. Two simulations were performed with the same substrate feeding but different realized values for the plant. In the plant simulation, the upper value was used, while in the model simulation, the nominal value was used. This scheme is illustrated in Figure 7, in which the controller is provided with full-state feedback from the simulated plant, which takes the upper value of the influent concentration as the realized value.

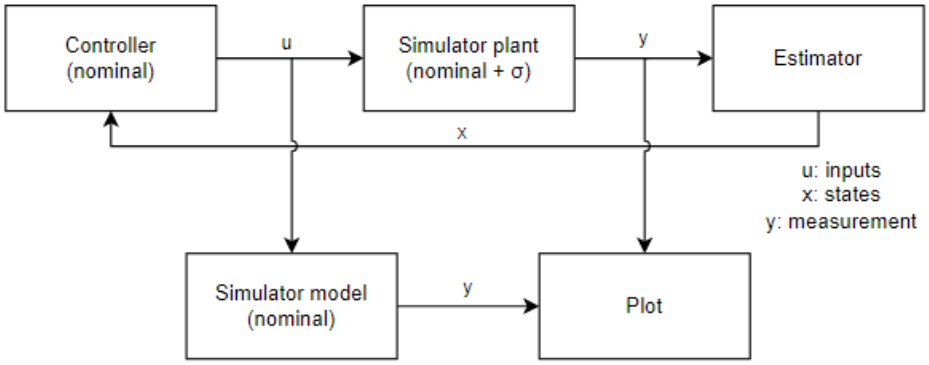

Figure 7. *Sensitivity analysis scheme.*

2.5.3 Plant-model mismatch implementation

To eliminate the randomness of the model, the plant was supplied only with the upper value of the carbohydrates bound. The other parameters were kept the same. The obtained values are presented in Table 1.

Table 1. *Substrate values used for carbohydrates in* $kg\,m^{-3}$

Substrate	**Nominal**	**Standard deviation** (σ)	**1** σ	**3** σ	**5** σ
Corn Silage	254.4	26.4	[225.9 to 278.8]	[173.1 to 331.6]	[120.3 to 384.5]
Grass Silage	188.1	15.0	[173.1 to 203.2]	[143.0 to 233.3]	[112.9 to 263.3]
Cattle Manure	29.0	3.2	[25.7 to 32.2]	[19.2 to 38.7]	[12.7 to 45.2]
Sugar Beet Silage	487.8	18.3	[469.5 to 506.0]	[433.0 to 542.6]	[396.5 to 579.1]

For the calculation of these standard deviations see Section 2.5.2.

For nominal MPC, the controller was supplied with the nominal value of the influent concentrations, while the plant realization uses the upper bound for the influent carbohydrates. In robust MPC, the controller receives both the upper and lower carbohydrate bounds, with the plant realization using the upper carbohydrate bound. The schemes for both control approaches are illustrated in Figure 8 and Figure 9.

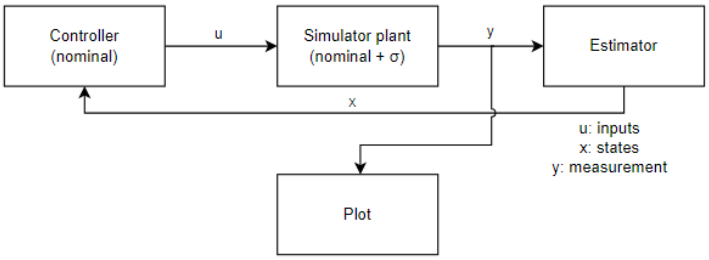

Figure 8. *Plant-model mismatch implemented on nominal MPC.*

Note that the controller only assumes the nominal value, resulting in only 1 scenario.

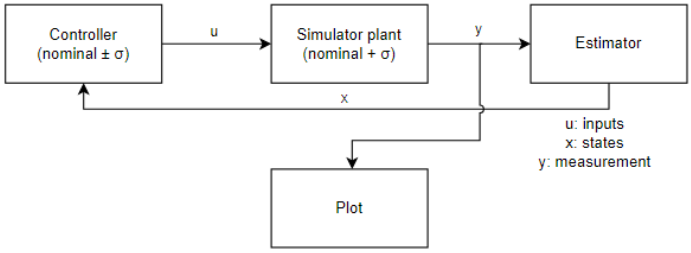

Figure 9. *Plant-model mismatch implemented on robust MPC.*

Note that the controller assumes the bounds of the concentrations, resulting in a scenario tree.

2.5.4 Time step ahead prediction

For each point in the $prediction\ horizon$, MPC predicts the system trajectory, which is computed based on the information the controller has received during the simulation at time t. In MPC, only the first entry of the optimal control trajectory is applied to the plant. As a result, the plant behaves differently than the model due to the plant-model mismatch; therefore, predicted and realized plant values differ. The values predicted for future times $t_1, t_2, \ldots, t_{N_{horizon}}$ by the controller at time t_0 are referred to as time step-ahead predictions. Figure 10 illustrates a scheme for a time step ahead prediction of 1, meaning that we get the prediction of t_{k+1} at time step t_k.

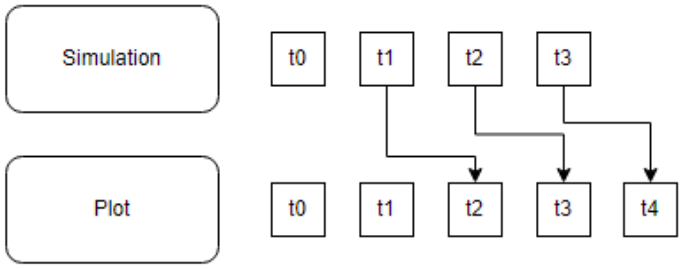

Figure 10. *Scheme of a time step ahead prediction of 1.*

3 Results and discussion

3.1 Methanation scenario

3.1.1 Ideal case

The methanation scenario with state feedback is run as an ideal case, meaning there is no plant-model mismatch, as the parameters on the plant and the model are kept the same. At each setpoint change, the fed substrates show peak feedings, indicating that the controller responds to the changes by delivering a large amount of a specific substrate over a short period. The controller increases production by feeding sugar beet silage or grass silage and decreases production by feeding cattle manure, mimicking an accelerator-brake mechanism, i.e. accelerating gas production through sugar beet silage and slowing it down through elevated volume flows of cattle manure.

This behavior is explained by the nominal values in Table 1, where sugar beet silage and grass silage have nominal values that are 10 times higher than those of cattle manure. Additionally, the high ammonia levels in cattle manure result in a temporary ammonia inhibition of the process, resulting in temporarily diminished gas production.

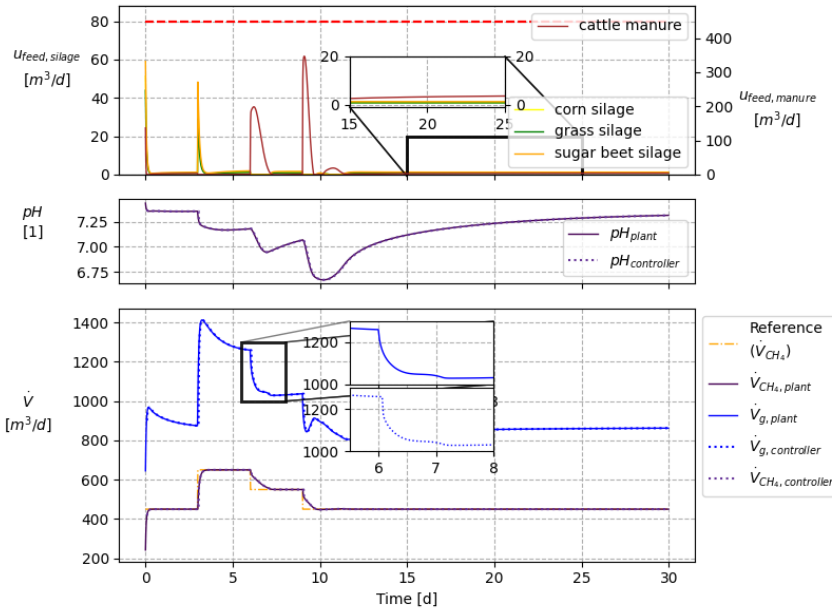

Figure 11. *Methanation scenario with nominal MPC and state feedback without mismatch. The prediction horizon is 15 time steps (7.5h), and the robust horizon is set to 0.*

During setpoint transitions, pH temporarily drops due to the sudden increase in substrate feeding, reaching a low of 6.75 before recovering to an optimal value near 7 when steady operation starts.

In this ideal case, perfect setpoint tracking and smooth methane flow transitions are observed with each setpoint change. Gas production shows peaks and valleys during transitions, especially on day 9, where a sharp increase in production stabilizes at 800 $m^3 d^{-1}$. Since this is an ideal scenario, the controller's predictions match the plant's realizations exactly. The results are illustrated in Figure 11.

3.1.2 Sensitivity analysis

Carbohydrates could be identified as the macronutrient that most significantly influenced gas production, compared with proteins and lipids. The results of the sensitivity analysis are shown in Figure 12, where the solid line represents the output obtained from the plant with the upper value for influent carbohydrates, and the dotted line represents the output of the plant model assuming the nominal value for influent carbohydrates for the same amount of substrate fed. The plant-model mismatch was set to 1 standard deviation.

Reasonably, the plant, assuming the higher influent carbohydrates, realizes a higher gas flow value than the plant assuming the nominal, and thus, lower influent carbohydrates. This difference leads to a discrepancy in both gas production and pH outputs. The result is presented in Figure 12. Note that even though the process went into pH inhibition, the insight of this sensitivity analysis is to compute the effect of different levels of influent carbohydrates on gas production.

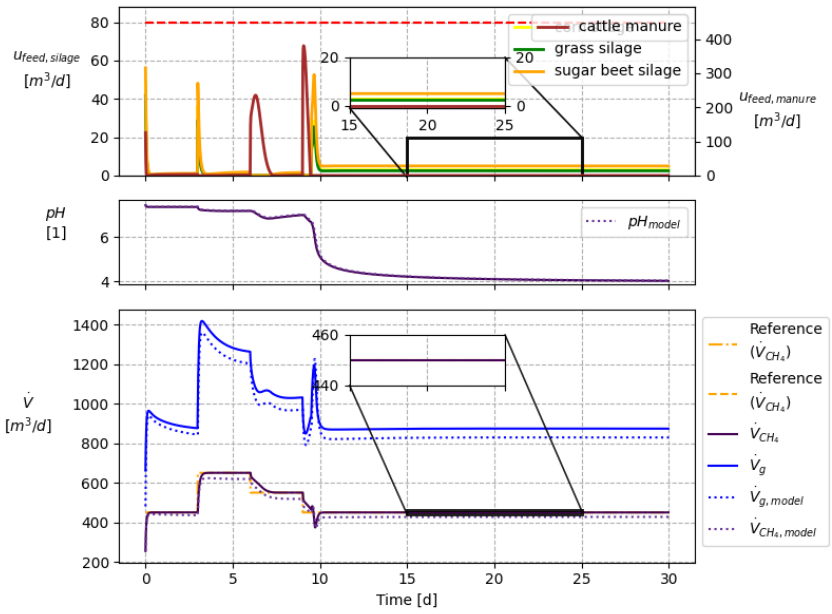

Figure 12. *Sensitivity analysis for carbohydrates in the methanation scenario with nominal MPC. The prediction horizon is 15-time steps (7.5h), and the robust horizon is set to 0.*

3.1.3 Nominal and Robust MPC

Nominal and robust MPC with state feedback were simulated for the methanation scenario, with a mismatch of 5 standard deviations, a prediction horizon of 15 time steps (7.5h), and a robust horizon of 0 for nominal MPC and 1 for robust MPC. In the nominal MPC case, setpoint tracking is generally good, but the transition on day 7 is not performed smoothly. Due to the plant-model mismatch, production peaks occur on day 7, reaching around 1500 $m^3 d^{-1}$. This sudden peak causes the pH to drop to an inhibition value of 4. It is worth mentioning that despite the low pH value, methane production was satisfied at the price of feeding more substrates. Since a time step-ahead prediction of 3 is used for plotting, the dotted lines resemble a controller that has an effective prediction horizon of 12 instead of the full horizon of 15.

Robust MPC, substrate peaks are less pronounced compared to the nominal case, resulting in smoother transitions between setpoints while maintaining good tracking performance. The pH oscillates between 7.5 and 7.2, avoiding inhibition throughout the operation. In the magnified view, we observe two distinct dotted lines for the robust case, indicating that the controller calculates two different trajectory paths, one for each scenario, i.e. each bound. This allows the controller to account for potential scenarios during the prediction horizon. As in the nominal case, a time step-ahead prediction of 3 is used for plotting, and the dotted lines resemble again a controller with an effective prediction horizon of 12.

For both nominal and robust MPC cases, it was observed that decreasing setpoints are tracked less precisely than increasing ones. This discrepancy may be related to the tuning parameters used in the controller, such as the cost associated with the individual substrate; as well as the nonlinear model structure, which allows increasing gas production easier than decreasing.

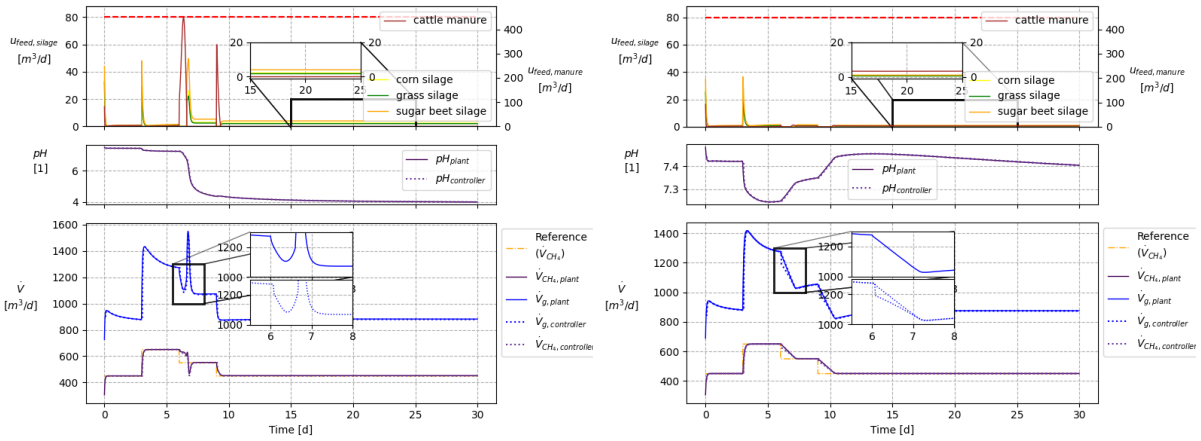

(a) *Nominal MPC (excerpt)* ***(b)*** *Robust MPC*

Figure 13. *Methanation scenario with state feedback and a mismatch of 5 standard deviations. The prediction horizon is 15 time steps (7.5h). The robust horizon is set to 0 for nominal MPC and 1 for robust MPC, with a time step-ahead prediction of 3*

3.2 Cogeneration scenario

3.2.1 Ideal case

The cogeneration scenario with state feedback was run as an ideal case. In this scenario, the gas storage tank bounds constraints are indicated by the red dashed lines in the middle plot of Figure 14. A safety margin of 5% is included, represented by the blue dashed lines at 19 and 365 m^3. In the ideal scenario, cattle manure and sugar beet silage are the primary substrates fed into the reactor, maintaining a storage level of about 40% and resulting in oscillating gas production between 250 and 450 $m^3 d^{-1}$.

The pH exhibited a mean value of 7.55, indicating that pH inhibition was not present in the system. Even though the maximum safe filling of the storage tanks was almost reached on days 21 and 26, and cattle manure was fed to the maximum allowed limit, no constraint violations occurred. The controller accurately predicted the system's output during operation, as there was no plant-model mismatch. The magnified views demonstrate that the controller's predictions align exactly with the plant's actual output.

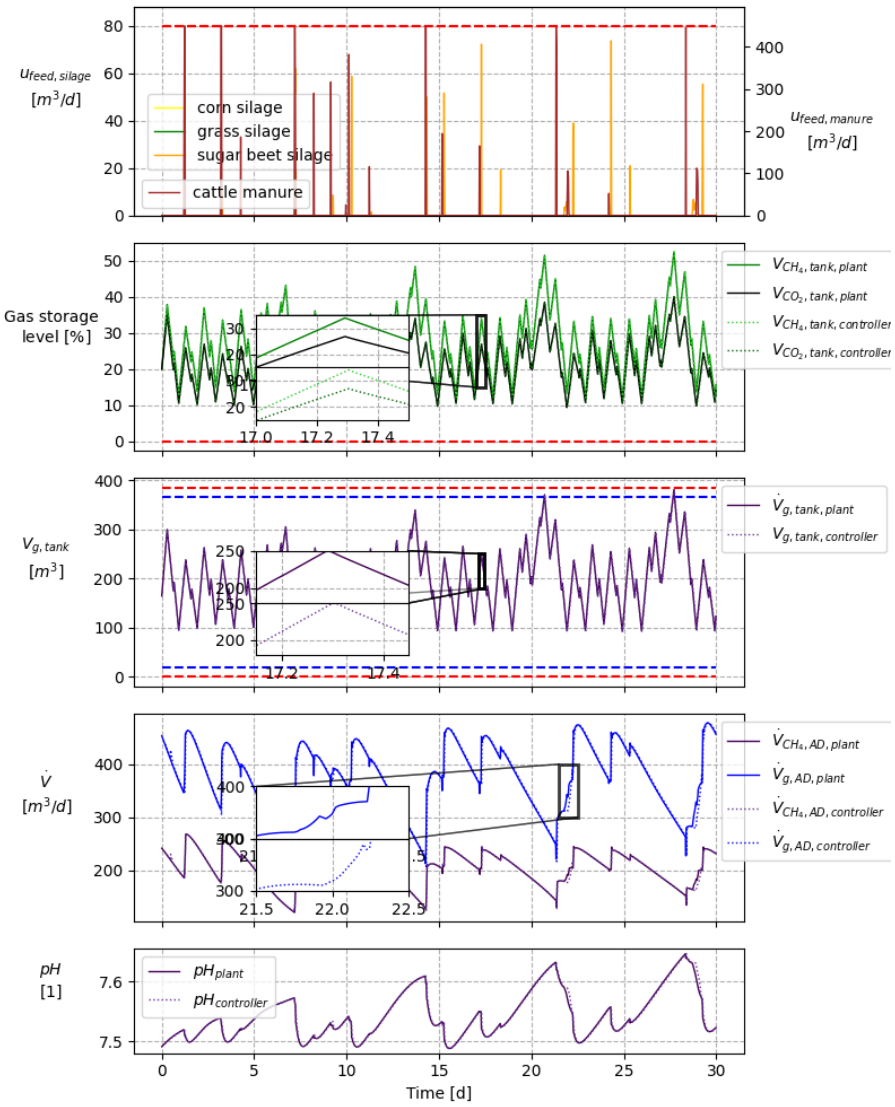

Figure 14. *Cogeneration scenario with nominal MPC and state feedback, without mismatch. The prediction horizon is 40 time steps (20h), and the robust horizon is 0.*

3.2.2 Nominal and Robust MPC

When a mismatch of 3 standard deviations is implemented, nominal MPC performs well until day 21, when the upper safety margin is violated, as shown in Figure 15a. However, on day 27 the gas production exceeds the hard constraint of the storage tank volume, leading to an infeasible state from which the system cannot recover. From day 27 onward, the plant realizes values outside the constraints and the controller feeds large amounts of all substrates in an attempt to minimize infeasibility.

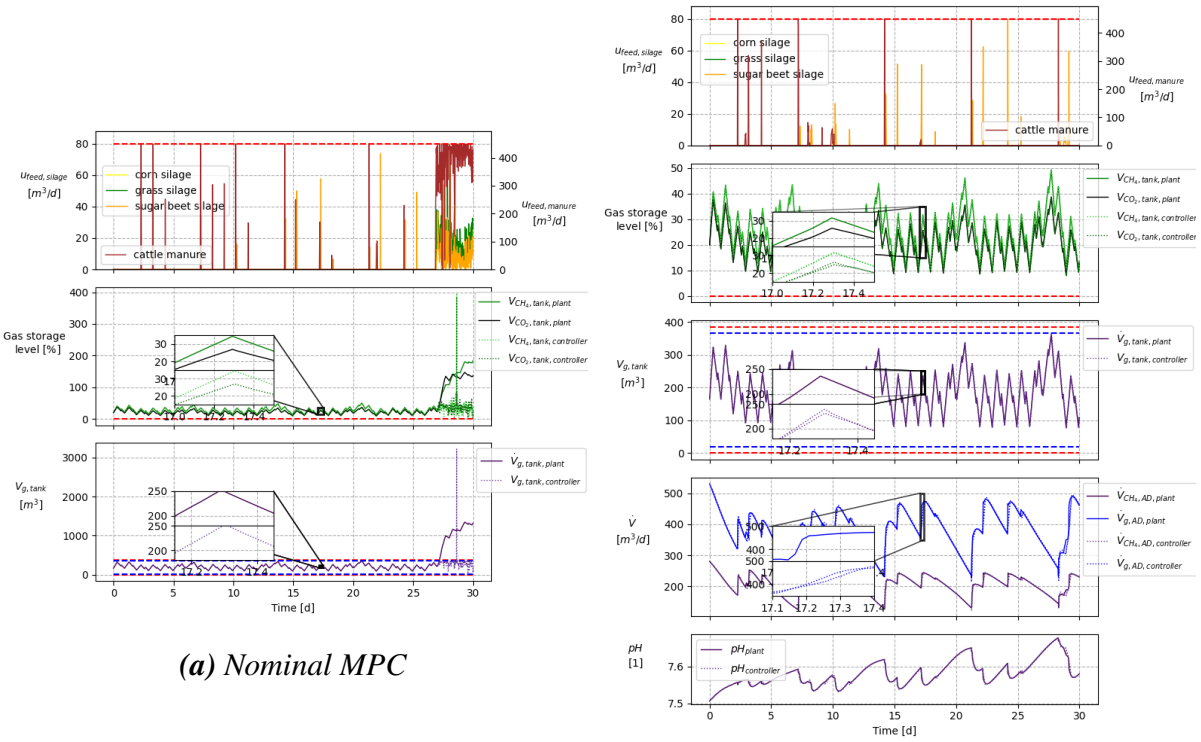

(a) *Nominal MPC*

(b) *Robust MPC*

Figure 15. *Methanation scenario with state feedback and a mismatch of 3 standard deviations. The prediction horizon is 40 time steps (20h). The robust horizon is 0 for nominal MPC and 1 for robust MPC, A time step ahead prediction of 8 is used for plotting.*

Note that despite the infeasibility, the controller predictions mostly remain within the constraints, except for the peak at day 28. Due to the plant-model mismatch, the actual gas production deviates from the intended result. By day 30, the final state of the simulation shows a volume of 1200 m³, which is 5 times greater than the actual volume.

In contrast to the results obtained with nominal MPC, robust MPC performs well throughout the entire operation. Constraints are not violated, and the pH maintains an average value of 7.6, avoiding inhibition. Robust MPC effectively manages the scenario by predicting both possible outcomes, maintaining a gas storage level of about 45% and an average gas production rate of approximately 400 $m^3 d^{-1}$. By forecasting potential violations and adjusting accordingly, robust MPC prevents constraint violations and ensures stable operation.

4 Conclusions

1. ADM1-R3-Core produces comparable results to the ADM1-R3 model. However, as states were removed, tuning parameters are introduced; the value of these parameters can modify the exactness and reliability of the model.
2. Carbohydrates significantly influence gas production in comparison to proteins, and lipids. Sensitivity analysis showed that discrepancies in influent carbohydrate values between the controller and the plant lead to differences in gas production and pH.
3. In the ideal case of no plant-model mismatch, nominal MPC achieves good setpoint tracking and smooth transitions. However, when a plant-model mismatch is introduced, nominal MPC struggles. This is particularly evident when constraint violation occurs, such as in the cogenerations scenario, causing infeasibility and significant deviations in gas production and pH levels between the prediction of the controller and the realized value of the plant.
4. Robust MPC performs better than nominal MPC when a plant-model mismatch is present. It manages constraints effectively, preventing violations by predicting the scenario outcomes and adjusting the control actions accordingly. Robust MPC maintains stable gas production and pH levels, even when a mismatch is present, at the price of increased computational load to account for the different scenarios.

Bibliography

Fiedler, F., Karg, B., Lüken, L., Brandner, D., Heinlein, M., Brabender, F., & Lucia, S. (2023). *Do-mpc: Towards fair nonlinear and robust model predictive control*. https://doi.org/https://doi.org/10.1016/j.conengprac.2023.105676

Frontzek, J. (2024). *Multi-stage mpc of agricultural biogas plants with uncertain substrate characterization* [Fakultät III Prozesswissenschaften, Institut Prozess- und Verfahrenstechnik, Chair of Control]. TU Berlin.

Graichen, K. (2024). *Numerical optimization and model predictive control* [Chair of Automatic Control]. Friedrich-Alexander-Universität.

Lougee, R. (2003). *The common optimization interface for operations research: Promoting open-source software in the operations research community*. https://doi.org/10.1147/rd.471.0057

Lucia, S., & Engell, S. (2014). *Control of towing kites under uncertainty using robust economic nonlinear model predictive control*. https://doi.org/10.1109/ECC.2014.6862335

Wächter, A., & Biegler, L. T. (2006). On the implementation of an interior-point filter line-search algorithm for large-scale nonlinear programming. *Math. Program*, *106*, 25–57. https://doi.org/https://doi.org/10.1007/s10107-004-0559-y

Weinrich, S. (2017). *Praxisnahe modellierung von biogasanlagen: Systematische vereinfachung des anaerobic digestion model no. 1 (ADM1)* (Doctoral dissertation). Universität Rostock. https://doi.org/10.18453/rosdok{\textunderscore}id00002016

Weinrich, S., & Nelles, M. (2021). Systematic simplification of the anaerobic digestion model no. 1 (adm1) – model development and stoichiometric analysis. *Bioresource Technology*, *333*, 125124. https://doi.org/https://doi.org/10.1016/j.biortech.2021.125124

A Appendix

The ADM1 simplifications of Weinrich and Nelles (2021) and by have been transformed into standard control notation. This section summarizes the model equations and parameters of all successfully investigated models, starting with the simplest model structures. The following notation was applied:

- x_i - states (mass concentrations of the species involved),
- y_i - measurements
- u - control variable (feed volume flow)
- ξ_i - time-variant, substrate-specific uncertain parameters (inlet mass concentrations)
- θ_i - time-variant parameters
- c_i - (aggregated) time-invariant parameters
- a_{ij} - time-invariant stoichiometric coefficients

States and inlet concentrations are usually given in kgm^3. The feed volume flow is stated in m³/d. Units of states, inputs and measurements are summarized in Table1. Units of all model parameters can be reviewed in (Weinrich, 2017).

Table 1. *Units of states, inputs and measurements of all described models.*

Symbol	Description	Unit
x_i	states	kg/m^3
ξ_i	inlet concentrations	kg/m^3
u	feed volume flow	m^3/d
V_{g}	biogas volume flow	m^3/d
p_{ch4}	partial pressure of methane	bar
p_{co2}	partial pressure of carbon dioxide	bar
pH	pH value	$-$
S_{IN}	inorganic nitrogen concentration	kg/m^3
TS	total solids content	$\%$-FM; $\mathrm{kg_{TS}}$ / $\mathrm{kg_{FM}}$
VS	volatile solids content	$\%$-TS; $\mathrm{kg_{VS}}$ / $\mathrm{kg_{TS}}$
S_{ac}	acetic acid concentration	kg/m^3

A.1 ADM1-R3

The ADM1-R3 contains more process information than the ADM1-R4. Its crucial components are the pH value as well as acetic acid as an intermediate product. Its concentration is a common indicator of process stability. Process inhibition in the event of too high acid concentrations is eventually caused by low pH values. Since pH drops can only be detected after all buffer capacity is consumed, measuring (or estimating) acetic acid concentrations is therefore critical for having an early warning indicator of possible process failure. State vector:

$$\begin{aligned}\boldsymbol{x} = [&S_{\mathrm{ac}}, S_{\mathrm{ch4}}, S_{\mathrm{IC}}, S_{\mathrm{IN}}, S_{\mathrm{h2o}}, X_{\mathrm{ch}}, X_{\mathrm{pr}}, X_{\mathrm{li}}, X_{\mathrm{bac}}, X_{\mathrm{ac}}, X_{\mathrm{ash}}, \dots \\ &S_{\mathrm{ion}}, S_{\mathrm{ac^-}}, S_{\mathrm{hco3^-}}, S_{\mathrm{nh3}}, S_{\mathrm{ch4,gas}}, S_{\mathrm{co2,gas}}]^T \end{aligned} \tag{A.1}$$

Differential equations:

$$x_1 = c_1\,(\xi_1 - x_1)\,u \;\; a_{11}\theta_1 x_6 \;\; a_{12}\theta_2 x_7 \;\; a_{13}\theta_3 x_8 - a_{14}\theta_5 \frac{x_1\,x_{10}}{\theta_6 \;\; x_1} I_{\mathrm{ac}} \tag{A.2a}$$

$$x_2 = c_1\,(\xi_2 - x_2)\,u \;\; a_{21}\theta_1 x_6 \;\; a_{22}\theta_2 x_7 \;\; a_{23}\theta_3 x_8 - c_5 x_2 \;\; c_6 x_{16} \;\; a_{24}\theta_5 \frac{x_1\,x_{10}}{\theta_7 \;\; x_1} I_{\mathrm{ac}} \tag{A.2b}$$

$$x_3 = c_1\,(\xi_3 - x_3)\,u \;\; a_{31}\theta_1 x_6 \;\; a_{32}\theta_2 x_7 - a_{33}\theta_3 x_8 - c_5 x_3 \;\; c_5 x_{14} \;\; c_7 x_{17} \;\; a_{34}\theta_5 \frac{x_1\,x_{10}}{\theta_6 \;\; x_1} I_{\mathrm{ac}} \tag{A.2c}$$

$$x_4 = c_1\,(\xi_4 - x_4)\,u - a_{41}\theta_1 x_6 \;\; a_{42}\theta_2 x_7 - a_{43}\theta_3 x_8 - a_{44}\theta_5 \frac{x_1\,x_{10}}{\theta_6 \;\; x_1} I_{\mathrm{ac}} \tag{A.2d}$$

$$x_5 = c_1\,(\xi_5 - x_5)\,u - a_{51}\theta_1 x_6 - a_{52}\theta_2 x_7 - a_{53}\theta_3 x_8 \;\; a_{54}\theta_5 \frac{x_1\,x_{10}}{\theta_6 \;\; x_1} I_{\mathrm{ac}} \tag{A.2e}$$

$$x_6 = c_1\,(\xi_6 - x_6)\,u - \theta_1 x_6 \;\; a_{65}\theta_4 x_9 \;\; a_{66}\theta_4 x_{10} \tag{A.2f}$$

$$x_7 = c_1\,(\xi_7 - x_7)\,u - \theta_2 x_7 \;\; a_{75}\theta_4 x_9 \;\; a_{76}\theta_4 x_{10} \tag{A.2g}$$

$$x_8 = c_1\,(\xi_8 - x_8)\,u - \theta_3 x_8 \;\; a_{85}\theta_4 x_9 \;\; a_{86}\theta_4 x_{10} \tag{A.2h}$$

$$x_9 = c_1\,(\xi_9 - x_9)\,u \;\; a_{91}\theta_1 x_6 \;\; a_{92}\theta_2 x_7 \;\; a_{93}\theta_3 x_8 - \theta_4 x_9 \tag{A.2i}$$

$$x_{10} = c_1\,(\xi_{10} - x_{10})\,u \;\; \theta_5 \frac{x_1\,x_{10}}{\theta_6 \;\; x_1} I_{\mathrm{ac}} - \theta_4 x_{10} \tag{A.2j}$$

$$x_{11} = c_1\,(\xi_{11} - x_{11})\,u \tag{A.2k}$$

$$x_{12} = c_1\,(\xi_{12} - x_{12})\,u \tag{A.2l}$$

$$x_{13} = c_{29}\,(x_1 - x_{13}) - c_9 x_{13} S_{\mathrm{H}} \tag{A.2m}$$

$$x_{14} = c_{30}\,(x_3 - x_{14}) - c_{10} x_{14} S_{\mathrm{H}} \tag{A.2n}$$

$$x_{15} = c_{31}\,(x_4 - x_{15}) - c_{11} x_{15} S_{\mathrm{H}} \tag{A.2o}$$

$$x_{16} = c_{22} x_{16}^3 \;\; c_{23} x_{16}^2 x_{17} \;\; c_{24} x_{16} x_{17}^2 \;\; c_{25} x_{16}^2 \;\; c_{26} x_{16} x_{17} \;\; c_{12} x_2 \;\; c_{27} x_{16} \tag{A.2p}$$

$$x_{17} = c_{24} x_{17}^3 \;\; c_{23} x_{16} x_{17}^2 \;\; c_{22} x_{16}^2 x_{17} \;\; c_{26} x_{17}^2 \;\; c_{25} x_{16} x_{17} \;\; c_{12} x_3 - c_{12} x_{14} \;\; c_{28} x_{17} \tag{A.2q}$$

I_{ac} and S_{H} are defined as

$$I_{\mathrm{ac}} = \frac{c_3}{c_3\ S_{\mathrm{H}}^{c_2}} \frac{x_4}{x_4\ c_8} \frac{\theta_7}{\theta_7\ x_{15}} \tag{A.3}$$

$$S_{\mathrm{H}} = -\frac{\Phi}{2}\ \frac{1}{2}\sqrt{\Phi^2\ c_4}\text{ , where} \tag{A.4}$$

$$\Phi = x_{12}\ \frac{x_4 - x_{15}}{17} - \frac{x_{14}}{44} - \frac{x_{13}}{60}. \tag{A.5}$$

The absolute values of the stoichiometric coefficients a_{ij} are given in the petersen matrix of ADM1-R3, Tab. 3. Note that for all ADM1-R3 models, definition and indexing of parameters and stoichiometric constants is independent from all ADM1-R4 models.

Measurements:

$$y_1 = V_{\mathrm{g}} = c_{13}x_{16}^2\ c_{14}x_{16}x_{17}\ c_{15}x_{17}^2\ c_{16}x_{16}\ c_{17}x_{17}\ c_{18} \tag{A.6a}$$

$$y_2 = p_{\mathrm{ch4}} = c_{19}x_{16} \tag{A.6b}$$

$$y_3 = p_{\mathrm{co2}} = c_{20}x_{17} \tag{A.6c}$$

$$y_4 = pH = -\log_{10} S_{\mathrm{H}} \tag{A.6d}$$

$$y_5 = S_{\mathrm{IN}} = x_4 \tag{A.6e}$$

$$y_6 = TS = 1 - \frac{1}{c_{21}}x_5, \tag{A.6f}$$

$$y_7 = VS = 1 - \frac{1}{c_{21} - x_5}x_{11} \tag{A.6g}$$

$$y_8 = S_{\mathrm{ac}} = x_1 \tag{A.6h}$$

Tab. 2 summarizes the aggregated parameters c_i and the time-variant parameters θ_i used for the ADM1-R3 models.

Table 2. *Aggregated and time-variant parameters and notation of ADM1-R3.*

Aggregated notation	Notation by Weinrich and Nelles (Weinrich & Nelles, 2021)
u	V_f
θ_1	k_{ch}
θ_2	k_{pr}
θ_3	k_{li}
θ_4	k_{dec}
θ_5	$\mu_{\mathrm{m,ac}}$

θ_6	$K_{\mathrm{S,ac}}$
θ_7	$K_{\mathrm{I,nh3}}$
θ_8	$\Delta S_{\mathrm{ion,eff}}$
θ_9	$\varphi_{\mathrm{IN,in}}$
c_1	V_{l}^{-1}
c_2	$n_{\mathrm{ac}} = 3\left(pH_{\mathrm{UL,ac}} - pH_{\mathrm{LL,ac}}\right)^{-1}$
c_3	$10^{-\frac{3}{2}\frac{pH_{\mathrm{UL,ac}} pH_{\mathrm{LL,ac}}}{pH_{\mathrm{UL,ac}} - pH_{\mathrm{LL,ac}}}}$
c_4	$4K_{\mathrm{W}}$
c_5	$k_{\mathrm{L}}a$
c_6	$k_{\mathrm{L}}a\, K_{\mathrm{H,ch4}}\bar{R}T$
c_7	$k_{\mathrm{L}}a\, K_{\mathrm{H,co2}}\bar{R}T$
c_8	$K_{\mathrm{S,IN}}$
c_9	$k_{\mathrm{AB,ac}}$
c_{10}	$k_{\mathrm{AB,co2}}$
c_{11}	$k_{\mathrm{AB,IN}}$
c_{12}	$k_{\mathrm{L}}a\, V_{\mathrm{l}}V_{\mathrm{g}}^{-1}$
c_{13}	$k_{\mathrm{p}}p_0^{-1}\left(\bar{R}T\bar{M}_{\mathrm{ch4}}^{-1}\right)^2$
c_{14}	$2k_{\mathrm{p}}p_0^{-1}\left(\bar{R}T\right)^2\bar{M}_{\mathrm{ch4}}^{-1}\bar{M}_{\mathrm{co2}}^{-1}$
c_{15}	$k_{\mathrm{p}}p_0^{-1}\left(\bar{R}T\bar{M}_{\mathrm{co2}}^{-1}\right)^2$
c_{16}	$k_{\mathrm{p}}p_0^{-1}\bar{R}T\bar{M}_{\mathrm{ch4}}^{-1}\left(2p_{\mathrm{h2o}} - p_0\right)$
c_{17}	$k_{\mathrm{p}}p_0^{-1}\bar{R}T\bar{M}_{\mathrm{co2}}^{-1}\left(2p_{\mathrm{h2o}} - p_0\right)$
c_{18}	$k_{\mathrm{p}}p_0^{-1}\left(p_{\mathrm{h2o}} - p_0\right)p_{\mathrm{h2o}}$
c_{19}	$\bar{R}T\bar{M}_{\mathrm{ch4}}^{-1}$
c_{20}	$\bar{R}T\bar{M}_{\mathrm{co2}}^{-1}$
c_{21}	ρ_{l}
c_{22}	$-k_{\mathrm{p}}V_{\mathrm{g}}^{-1}p_0^{-1}\left(\bar{R}T\bar{M}_{\mathrm{ch4}}^{-1}\right)^2$
c_{23}	$-2k_{\mathrm{p}}V_{\mathrm{g}}^{-1}p_0^{-1}\left(\bar{R}T\right)^2\bar{M}_{\mathrm{ch4}}^{-1}\bar{M}_{\mathrm{co2}}^{-1}$
c_{24}	$-k_{\mathrm{p}}V_{\mathrm{g}}^{-1}p_0^{-1}\left(\bar{R}T\bar{M}_{\mathrm{co2}}^{-1}\right)^2$
c_{25}	$-k_{\mathrm{p}}V_{\mathrm{g}}^{-1}p_0^{-1}\bar{R}T\bar{M}_{\mathrm{ch4}}^{-1}\left(2p_{\mathrm{h2o}} - p_0\right)$
c_{26}	$-k_{\mathrm{p}}V_{\mathrm{g}}^{-1}p_0^{-1}\bar{R}T\bar{M}_{\mathrm{co2}}^{-1}\left(2p_{\mathrm{h2o}} - p_0\right)$
c_{27}	$-k_{\mathrm{L}}a\, V_{\mathrm{l}}V_{\mathrm{g}}^{-1}K_{\mathrm{H,ch4}}\bar{R}T - k_{\mathrm{p}}V_{\mathrm{g}}^{-1}p_0^{-1}\left(p_{\mathrm{h2o}} - p_0\right)p_{\mathrm{h2o}}$
c_{28}	$-k_{\mathrm{L}}a\, V_{\mathrm{l}}V_{\mathrm{g}}^{-1}K_{\mathrm{H,co2}}\bar{R}T - k_{\mathrm{p}}V_{\mathrm{g}}^{-1}p_0^{-1}\left(p_{\mathrm{h2o}} - p_0\right)p_{\mathrm{h2o}}$

c_{29}	$k_{\mathrm{AB,ac}} K_{\mathrm{a,ac}}$
c_{30}	$k_{\mathrm{AB,co2}} K_{\mathrm{a,co2}}$
c_{31}	$k_{\mathrm{AB,IN}} K_{\mathrm{a,IN}}$
c_{32}	$V_{\mathrm{l}} V_{\mathrm{g}}^{-1}$

Normalized ADM1-R3

Normalization is performed with arbitrary values for states x, outputs y and inputs u, for instance with the steady-state values. General notation of the normalization matrices is as follows:

$$\boldsymbol{x} = \boldsymbol{T_x}\bar{\boldsymbol{x}}, \tag{A.7a}$$

$$\boldsymbol{y} = \boldsymbol{T_y}\bar{\boldsymbol{y}}, \tag{A.7b}$$

$$\boldsymbol{u} = \boldsymbol{T_u}\bar{\boldsymbol{u}}, \tag{A.7c}$$

where $\bar{\boldsymbol{x}}, \bar{\boldsymbol{y}}$, and $\bar{\boldsymbol{u}}$ are the normalized coordinates. For single-input systems, (A.7c) reduces to a scalar expression:

$$u = T_u \bar{u}. \tag{A.8}$$

Accordingly, inlet concentrations are normalized with the same matrix as the states:

$$\boldsymbol{\xi} = \boldsymbol{T_x}\bar{\boldsymbol{\xi}}. \tag{A.9}$$

Normalized state differential equations:

$$\begin{aligned}
\bar{x}_1 = {} & c_1 \left(\bar{\xi}_1 - \bar{x}_1\right) T_u\, \bar{u}\ \ a_{1,1}\theta_1 \frac{T_{x,6}}{T_{x,1}} \bar{x}_6\ \ a_{1,2}\theta_2 \frac{T_{x,7}}{T_{x,1}} \bar{x}_7\ \ a_{1,3}\theta_3 \frac{T_{x,8}}{T_{x,1}} \bar{x}_8 \\
& - a_{1,4}\theta_5 T_{x,11} \frac{\bar{x}_1\, \bar{x}_{10}}{\theta_6\ T_{x,1} \bar{x}_1} \bar{I}_{\mathrm{ac}}
\end{aligned} \tag{A.10a}$$

$$\begin{aligned}
\bar{x}_2 = {} & c_1 \left(\bar{\xi}_2 - \bar{x}_2\right) T_u\, \bar{u}\ \ a_{2,1}\theta_1 \frac{T_{x,6}}{T_{x,2}} \bar{x}_6\ \ a_{2,2}\theta_2 \frac{T_{x,7}}{T_{x,2}} \bar{x}_7\ \ a_{2,3}\theta_3 \frac{T_{x,8}}{T_{x,2}} \bar{x}_8 \\
& a_{2,4}\theta_5 \frac{T_{x,1}\, T_{x,10}}{T_{x,2}} \frac{\bar{x}_1\, \bar{x}_{10}}{\theta_6\ T_{x,1} \bar{x}_1} \bar{I}_{\mathrm{ac}} - c_5 \bar{x}_2\ \ c_6 \frac{T_{x,16}}{T_{x,2}} \bar{x}_{16}
\end{aligned} \tag{A.10b}$$

$$\begin{aligned}
\bar{x}_3 = {} & c_1 \left(\bar{\xi}_3 - \bar{x}_3\right) T_u\, \bar{u}\ \ a_{3,1}\theta_1 \frac{T_{x,6}}{T_{x,3}} \bar{x}_6\ \ a_{3,2}\theta_2 \frac{T_{x,7}}{T_{x,3}} \bar{x}_7 - a_{3,3}\theta_3 \frac{T_{x,8}}{T_{x,3}} \bar{x}_8 \\
& a_{3,4}\theta_5 \frac{T_{x,1}\, T_{x,10}}{T_{x,3}} \frac{\bar{x}_1\, \bar{x}_{10}}{\theta_6\ T_{x,1} \bar{x}_1} \bar{I}_{\mathrm{ac}} - c_5 \bar{x}_3\ \ c_5 \frac{T_{x,14}}{T_{x,3}} \bar{x}_{14}\ \ c_7 \frac{T_{x,17}}{T_{x,3}} \bar{x}_{17}
\end{aligned} \tag{A.10c}$$

$$\bar{x}_4 = c_1 \left(\bar{\xi}_4 - \bar{x}_4\right) T_u\, \bar{u} - a_{4,1}\theta_1 \frac{T_{x,6}}{T_{x,4}} \bar{x}_6\ \ a_{4,2}\theta_2 \frac{T_{x,7}}{T_{x,4}} \bar{x}_7 - a_{4,3}\theta_3 \frac{T_{x,8}}{T_{x,4}} \bar{x}_8$$

$$- a_{4,4}\theta_5\frac{T_{x,1}\,T_{x,10}}{T_{x,4}}\frac{\bar{x}_1\,\bar{x}_{10}}{\theta_6\;\;T_{x,1}\bar{x}_1}\bar{I}_{\mathrm{ac}} \tag{A.10d}$$

$$\bar{x}_5 = c_1\left(\bar{\xi}_5 - \bar{x}_5\right)T_u\,\bar{u} - a_{5,1}\theta_1\frac{T_{x,6}}{T_{x,5}}\bar{x}_6 - a_{5,2}\theta_2\frac{T_{x,7}}{T_{x,5}}\bar{x}_7 - a_{5,3}\theta_3\frac{T_{x,8}}{T_{x,5}}\bar{x}_8$$
$$a_{5,4}\theta_5\frac{T_{x,1}\,T_{x,10}}{T_{x,5}}\frac{\bar{x}_1\,\bar{x}_{10}}{\theta_6\;\;T_{x,1}\bar{x}_1}\bar{I}_{\mathrm{ac}} \tag{A.10e}$$

$$\bar{x}_6 = c_1\left(\bar{\xi}_6 - \bar{x}_6\right)T_u\,\bar{u} - \theta_1\bar{x}_6\;\;a_{6,5}\theta_4\frac{T_{x,9}}{T_{x,6}}\bar{x}_9\;\;a_{6,6}\theta_4\frac{T_{x,10}}{T_{x,6}}\bar{x}_{10} \tag{A.10f}$$

$$\bar{x}_7 = c_1\left(\bar{\xi}_7 - \bar{x}_7\right)T_u\,\bar{u} - \theta_2\bar{x}_7\;\;a_{7,5}\theta_4\frac{T_{x,9}}{T_{x,7}}\bar{x}_9\;\;a_{7,6}\theta_4\frac{T_{x,10}}{T_{x,7}}\bar{x}_{10} \tag{A.10g}$$

$$\bar{x}_8 = c_1\left(\bar{\xi}_8 - \bar{x}_8\right)T_u\,\bar{u} - \theta_3\bar{x}_8\;\;a_{8,5}\theta_4\frac{T_{x,9}}{T_{x,8}}\bar{x}_9\;\;a_{8,6}\theta_4\frac{T_{x,10}}{T_{x,8}}\bar{x}_{10} \tag{A.10h}$$

$$\bar{x}_9 = c_1\left(\bar{\xi}_9 - \bar{x}_9\right)T_u\,\bar{u}\;\;a_{9,1}\theta_1\frac{T_{x,6}}{T_{x,9}}\bar{x}_6\;\;a_{9,2}\theta_2\frac{T_{x,7}}{T_{x,9}}\bar{x}_7\;\;a_{9,3}\theta_3\frac{T_{x,8}}{T_{x,9}}\bar{x}_8 - \theta_4\bar{x}_9 \tag{A.10i}$$

$$\bar{x}_{10} = c_1\left(\bar{\xi}_{10} - \bar{x}_{10}\right)T_u\,\bar{u}\;\;\theta_5 T_{x,1}\frac{\bar{x}_1\,\bar{x}_{10}}{\theta_6\;\;T_{x,1}\bar{x}_1}\bar{I}_{\mathrm{ac}} - \theta_4\bar{x}_{10} \tag{A.10j}$$

$$\bar{x}_{11} = c_1\left(\bar{\xi}_{11} - \bar{x}_{11}\right)T_u\,\bar{u} \tag{A.10k}$$

$$\bar{x}_{12} = c_1\left(\bar{\xi}_{12} - \bar{x}_{12}\right)T_u\,\bar{u} \tag{A.10l}$$

$$\bar{x}_{13} = c_{29}\left(\frac{T_{x,1}}{T_{x,13}}\bar{x}_1 - \bar{x}_{13}\right) - c_9\bar{x}_{13}\bar{S}_{\mathrm{H}} \tag{A.10m}$$

$$\bar{x}_{14} = c_{30}\left(\frac{T_{x,3}}{T_{x,14}}\bar{x}_3 - \bar{x}_{14}\right) - c_{10}\bar{x}_{14}\bar{S}_{\mathrm{H}} \tag{A.10n}$$

$$\bar{x}_{15} = c_{31}\left(\frac{T_{x,4}}{T_{x,15}}\bar{x}_4 - \bar{x}_{15}\right) - c_{11}\bar{x}_{15}\bar{S}_{\mathrm{H}} \tag{A.10o}$$

$$\bar{x}_{16} = c_{22}T_{x,16}^2\,\bar{x}_{16}^3\;\;c_{23}T_{x,16}\,T_{x,17}\,\bar{x}_{16}^2\bar{x}_{17}\;\;c_{24}T_{x,17}^2\,\bar{x}_{16}\bar{x}_{17}^2\;\;c_{25}T_{x,16}\,\bar{x}_{16}^2\;\;c_{26}T_{x,17}\,\bar{x}_{16}\bar{x}_{17}$$
$$c_{12}\frac{T_{x,2}}{T_{x,16}}\,\bar{x}_2\;\;c_{27}\bar{x}_{16} \tag{A.10p}$$

$$\bar{x}_{17} = c_{24}T_{x,17}^2\,\bar{x}_{17}^3\;\;c_{23}T_{x,16}\,T_{x,17}\,\bar{x}_{16}\bar{x}_{17}^2\;\;c_{22}T_{x,16}^2\,\bar{x}_{16}^2\bar{x}_{17}\;\;c_{26}T_{x,17}\,\bar{x}_{17}^2\;\;c_{25}T_{x,16}\,\bar{x}_{16}\bar{x}_{17}$$
$$c_{12}\frac{T_{x,3}}{T_{x,17}}\,\bar{x}_3 - c_{12}\frac{T_{x,14}}{T_{x,17}}\,\bar{x}_{14}\;\;c_{28}\bar{x}_{17} \tag{A.10q}$$

Therein, $\bar{I}_{\mathrm{ac}}$ and $\bar{S}_{\mathrm{H}}$ are defined as

$$\bar{I}_{\mathrm{ac}} = \frac{c_3}{c_3\;\;\bar{S}_{\mathrm{H}}^{c_2}}\frac{\bar{x}_4}{\bar{x}_4\;\;c_8T_{x,4}}\frac{\theta_7}{\theta_7\;\;T_{x,15}\,\bar{x}_{15}} \tag{A.11}$$

$$\bar{S}_{\mathrm{H}} = -\frac{\bar{\mathbf{\Phi}}}{2}\;\;\frac{1}{2}\sqrt{\bar{\mathbf{\Phi}}^2\;\;c_4}\text{ , where} \tag{A.12}$$

$$\bar{\mathbf{\Phi}} = T_{x,12}\,\bar{x}_{12}\;\;\frac{T_{x,4}\,\bar{x}_4 - T_{x,15}\,\bar{x}_{15}}{17} - \frac{T_{x,14}\,\bar{x}_{14}}{44} - \frac{T_{x,13}\,\bar{x}_{13}}{60}. \tag{A.13}$$

Normalized measurements:

$$\bar{y}_1 = c_{13}\frac{T_{x,16}^2}{T_{y,1}}\,\bar{x}_{16}^2\;\; c_{14}\frac{T_{x,16}\,T_{x,17}}{T_{y,1}}\,\bar{x}_{16}\bar{x}_{17}\;\; c_{15}\frac{T_{x,17}^2}{T_{y,1}}\,\bar{x}_{17}^2\;\; c_{16}\frac{T_{x,16}}{T_{y,1}}\,\bar{x}_{16} \\ c_{17}\frac{T_{x,17}}{T_{y,1}}\,\bar{x}_{17}\;\; \frac{c_{18}}{T_{y,1}} \tag{A.14a}$$

$$\bar{y}_2 = c_{19}\frac{T_{x,16}}{T_{y,2}}\,\bar{x}_{16} \tag{A.14b}$$

$$\bar{y}_3 = c_{20}\frac{T_{x,17}}{T_{y,3}}\,\bar{x}_{17} \tag{A.14c}$$

$$\bar{y}_4 = -T_{y,4}^{-1}\,\log_{10}\bar{S}_{\mathrm{H}} \tag{A.14d}$$

$$\bar{y}_5 = \frac{T_{x,4}}{T_{y,5}}\,\bar{x}_4 \tag{A.14e}$$

$$\bar{y}_6 = T_{y,6}^{-1}\left(1 - \frac{T_{x,5}}{c_{21}}\bar{x}_5\right) \tag{A.14f}$$

$$\bar{y}_7 = T_{y,7}^{-1}\left(1 - \frac{T_{x,11}}{c_{21} - T_{x,5}\,\bar{x}_5}\bar{x}_{11}\right) \tag{A.14g}$$

$$\bar{y}_8 = \frac{T_{x,1}}{T_{y,8}}\bar{x}_1 \tag{A.14h}$$

Table 3. *Petersen matrix of ADM1-R3, derived from Weinrich (2017).*

Component i →	1	2	3	4	5	6	7	8	9	10	
j Process ↓	S_{ac}	S_{ch4}	S_{IC}	S_{IN}	S_{h2o}	X_{ch}	X_{pr}	X_{li}	X_{bac}	X_{ac}	**Process rate** r_j
1 Fermentation X_{ch}	0.6555	0.0818	0.2245	-0.0169	-0.0574	-1			0.1125		$\theta_1\, x_6$
2 Fermentation X_{pr}	0.9947	0.0696	0.1029	0.1746	-0.4767		-1		0.1349		$\theta_2\, x_7$
3 Fermentation X_{li}	1.7651	0.1913	-0.6472	-0.0244	-0.4470			-1	0.1621		$\theta_3\, x_8$
4 Methanogenesis S_{ac}	-26.5447	6.7367	18.4808	-0.1506	0.4778					1	$\theta_5\, \frac{x_1}{\theta_6 x_1}\, x_{10}\, I_{ac}$
5 Decay X_{bac}						0.18	0.77	0.05	-1		$\theta_4\, x_9$
6 Decay X_{ac}						0.18	0.77	0.05		-1	$\theta_4\, x_{10}$

	2	3	...	11	12	13	14	15	16	17	
	S_{ch4}	S_{IC}		X_{ash}	S_{ion}	$S_{\mathrm{ac-}}$	$S_{\mathrm{hco3-}}$	S_{nh3}	$S_{\mathrm{ch4,gas}}$	$S_{\mathrm{co2,gas}}$	
7 Dissoziation S_{ac}						-1					$c_{29}\, x_{13} - x_1\;\; c_9\, x_{13}\, S_{\mathrm{H}}$
8 Dissoziation S_{IC}							-1				$c_{30}\, x_{14} - x_3\;\; c_{10}\, x_{14}\, S_{\mathrm{H}}$
9 Dissoziation S_{IN}								-1			$c_{31}\, x_{15} - x_4\;\; c_{11}\, x_{15}\, S_{\mathrm{H}}$
10 Phase transition S_{ch4}	-1								c_{32}		$c_5\, x_2 - c_6\, x_{16}$
11 Phase transition S_{co2}		-1								c_{32}	$c_5\, x_3 - x_{14} - c_7\, x_{17}$

ADM1-R3-Core

The ADM1-R3-Core neglects individual states of ash and water. Additionally, the state of free ions is replaced by a time-variant parameter to ensure successful model calibration. Moreover, the influent concentration of inorganic nitrogen is multiplied by a scaling factor $\varphi_{IN,in}$ to account for proper pH fitting, treated as the time-variant parameter θ_9. The state vector reads:

$$\boldsymbol{x} = [S_{\mathrm{ac}}, S_{\mathrm{ch4}}, S_{\mathrm{IC}}, S_{\mathrm{IN}}, X_{\mathrm{ch}}, X_{\mathrm{pr}}, X_{\mathrm{li}}, X_{\mathrm{bac}}, X_{\mathrm{ac}}, S_{\mathrm{ac^-}}, S_{\mathrm{hco3^-}}, S_{\mathrm{nh3}}, S_{\mathrm{ch4,gas}}, S_{\mathrm{co2,gas}}]^T. \tag{A.15}$$

Differential equations:

$$x_1 = c_1\,(\xi_1 - x_1)\,u\;\; a_{11}\theta_1 x_5\;\; a_{12}\theta_2 x_6\;\; a_{13}\theta_3 x_7\;\; a_{14}\theta_5 \frac{x_1\,x_9}{\theta_6\;\; x_1} I_{\mathrm{ac}} \tag{A.16a}$$

$$x_2 = c_1\,(\xi_2 - x_2)\,u\;\; a_{21}\theta_1 x_5\;\; a_{22}\theta_2 x_6\;\; a_{23}\theta_3 x_7 - c_5 x_2\;\; c_6 x_{13}\;\; a_{24}\theta_5 \frac{x_1\,x_9}{\theta_6\;\; x_1} I_{\mathrm{ac}} \tag{A.16b}$$

$$x_3 = c_1\,(\xi_3 - x_3)\,u\;\; a_{31}\theta_1 x_5\;\; a_{32}\theta_2 x_6\;\; a_{33}\theta_3 x_7 - c_5 x_3\;\; c_5 x_{11}\;\; c_7 x_{14}\;\; a_{34}\theta_5 \frac{x_1\,x_9}{\theta_6\;\; x_1} I_{\mathrm{ac}} \tag{A.16c}$$

$$x_4 = c_1\,(\xi_4\,\theta_9 - x_4)\,u\;\; a_{41}\theta_1 x_5\;\; a_{42}\theta_2 x_6\;\; a_{43}\theta_3 x_7\;\; a_{44}\theta_5 \frac{x_1\,x_9}{\theta_6\;\; x_1} I_{\mathrm{ac}} \tag{A.16d}$$

$$x_5 = c_1\,(\xi_5 - x_5)\,u - \theta_1 x_5\;\; a_{55}\theta_4 x_8\;\; a_{56}\theta_4 x_9 \tag{A.16e}$$

$$x_6 = c_1\,(\xi_6 - x_6)\,u - \theta_2 x_6\;\; a_{65}\theta_4 x_8\;\; a_{66}\theta_4 x_9 \tag{A.16f}$$

$$x_7 = c_1\,(\xi_7 - x_7)\,u - \theta_3 x_7\;\; a_{75}\theta_4 x_8\;\; a_{76}\theta_4 x_9 \tag{A.16g}$$

$$x_8 = c_1\,(\xi_8 - x_8)\,u\;\; a_{81}\theta_1 x_5\;\; a_{82}\theta_2 x_6\;\; a_{83}\theta_3 x_7 - \theta_4 x_8 \tag{A.16h}$$

$$x_9 = c_1\,(\xi_9 - x_9)\,u\;\; \theta_5 \frac{x_1\,x_9}{\theta_6\;\; x_1} I_{\mathrm{ac}} - \theta_4 x_9 \tag{A.16i}$$

$$x_{10} = c_{29}\,(x_1 - x_{10}) - c_9 x_{10} S_{\mathrm{H}} \tag{A.16j}$$

$$x_{11} = c_{30}\,(x_3 - x_{11}) - c_{10} x_{11} S_{\mathrm{H}} \tag{A.16k}$$

$$x_{12} = c_{31}\,(x_4 - x_{12}) - c_{11} x_{12} S_{\mathrm{H}} \tag{A.16l}$$

$$x_{13} = c_{22} x_{13}^3\;\; c_{23} x_{13}^2 x_{14}\;\; c_{24} x_{13} x_{14}^2\;\; c_{25} x_{13}^2\;\; c_{26} x_{13} x_{14}\;\; c_{12} x_2\;\; c_{27} x_{13} \tag{A.16m}$$

$$x_{14} = c_{24} x_{14}^3\;\; c_{23} x_{13} x_{14}^2\;\; c_{22} x_{13}^2 x_{14}\;\; c_{26} x_{14}^2\;\; c_{25} x_{13} x_{14}\;\; c_{12} x_3 - c_{12} x_{11}\;\; c_{28} x_{14} \tag{A.16n}$$

I_{ac} and S_{H} are defined as

$$I_{\mathrm{ac}} = \frac{c_3}{c_3\;\; S_{\mathrm{H}}^{c_2}} \frac{x_4}{x_4\;\; c_8} \frac{\theta_7}{\theta_7\;\; x_{12}} \tag{A.17}$$

$$S_{\mathrm{H}} = -\frac{\Phi}{2}\;\; \frac{1}{2}\sqrt{\Phi^2\;\; c_4}\text{ , where} \tag{A.18}$$

$$\Phi = \theta_8\;\; \frac{x_4 - x_{12}}{17} - \frac{x_{11}}{44} - \frac{x_{10}}{60}. \tag{A.19}$$

The absolute values of the stoichiometric coefficients a_{ij} are given in the petersen matrix of ADM1-R3-Core, Tab. 4. Note that for all ADM1-R3 models, definition and indexing of parameters and stoichiometric constants is independent from all ADM1-R4 models.

Measurements:

$$y_1 = V_\mathrm{g} = c_{13} x_{13}^2 \;\; c_{14} x_{13} x_{14} \;\; c_{15} x_{14}^2 \;\; c_{16} x_{13} \;\; c_{17} x_{14} \;\; c_{18} \tag{A.20a}$$

$$y_2 = p_\mathrm{ch4} = c_{19} x_{13} \tag{A.20b}$$

$$y_3 = p_\mathrm{co2} = c_{20} x_{14} \tag{A.20c}$$

$$y_4 = pH = -\log_{10} S_\mathrm{H} \tag{A.20d}$$

$$y_5 = S_\mathrm{IN} = x_4 \tag{A.20e}$$

$$y_6 = S_\mathrm{ac} = x_1 \tag{A.20f}$$

Normalized ADM1-R3-Core

Normalization is performed in line with (A.7). Normalized state differential equations:

$$\begin{aligned}\bar{x}_1 = {} & c_1 \left(\bar{\xi}_1 - \bar{x}_1\right) T_u \, \bar{u} \;\; a_{1,1}\theta_1 \frac{T_{x,5}}{T_{x,1}} \bar{x}_5 \;\; a_{1,2}\theta_2 \frac{T_{x,6}}{T_{x,1}} \bar{x}_6 \;\; a_{1,3}\theta_3 \frac{T_{x,7}}{T_{x,1}} \bar{x}_7 \\ & a_{1,4}\theta_5 T_{x,9} \frac{\bar{x}_1 \, \bar{x}_9}{\theta_6 \;\; T_{x,1}\bar{x}_1} \bar{I}_\mathrm{ac}\end{aligned} \tag{A.21a}$$

$$\begin{aligned}\bar{x}_2 = {} & c_1 \left(\bar{\xi}_2 - \bar{x}_2\right) T_u \, \bar{u} \;\; a_{2,1}\theta_1 \frac{T_{x,5}}{T_{x,2}} \bar{x}_5 \;\; a_{2,2}\theta_2 \frac{T_{x,6}}{T_{x,2}} \bar{x}_6 \;\; a_{2,3}\theta_3 \frac{T_{x,7}}{T_{x,2}} \bar{x}_7 \\ & - c_5 \bar{x}_2 \;\; c_6 \frac{T_{x,13}}{T_{x,2}} \bar{x}_{13} \;\; a_{2,4}\theta_5 \frac{T_{x,1} \, T_{x,9}}{T_{x,2}} \frac{\bar{x}_1 \, \bar{x}_9}{\theta_6 \;\; T_{x,1}\bar{x}_1} \bar{I}_\mathrm{ac}\end{aligned} \tag{A.21b}$$

$$\begin{aligned}\bar{x}_3 = {} & c_1 \left(\bar{\xi}_3 - \bar{x}_3\right) T_u \, \bar{u} \;\; a_{3,1}\theta_1 \frac{T_{x,5}}{T_{x,3}} \bar{x}_5 \;\; a_{3,2}\theta_2 \frac{T_{x,6}}{T_{x,3}} \bar{x}_6 \;\; a_{3,3}\theta_3 \frac{T_{x,7}}{T_{x,3}} \bar{x}_7 \\ & - c_5 \bar{x}_3 \;\; c_5 \frac{T_{x,11}}{T_{x,3}} \bar{x}_{11} \;\; c_7 \frac{T_{x,14}}{T_{x,3}} \bar{x}_{14} \;\; a_{3,4}\theta_5 \frac{T_{x,1} \, T_{x,9}}{T_{x,3}} \frac{\bar{x}_1 \, \bar{x}_9}{\theta_6 \;\; T_{x,1}\bar{x}_1} \bar{I}_\mathrm{ac}\end{aligned} \tag{A.21c}$$

$$\begin{aligned}\bar{x}_4 = {} & c_1 \left(\bar{\xi}_4 \, \theta_9 - \bar{x}_4\right) T_u \, \bar{u} \;\; a_{4,1}\theta_1 \frac{T_{x,5}}{T_{x,4}} \bar{x}_5 \;\; a_{4,2}\theta_2 \frac{T_{x,6}}{T_{x,4}} \bar{x}_6 \;\; a_{4,3}\theta_3 \frac{T_{x,7}}{T_{x,4}} \bar{x}_7 \\ & a_{4,4}\theta_5 \frac{T_{x,1} \, T_{x,9}}{T_{x,4}} \frac{\bar{x}_1 \, \bar{x}_9}{\theta_6 \;\; T_{x,1}\bar{x}_1} \bar{I}_\mathrm{ac}\end{aligned} \tag{A.21d}$$

$$\bar{x}_5 = c_1 \left(\bar{\xi}_5 - \bar{x}_5\right) T_u \, \bar{u} - \theta_1 \bar{x}_5 \;\; a_{5,5}\theta_4 \frac{T_{x,8}}{T_{x,5}} \bar{x}_8 \;\; a_{5,6}\theta_4 \frac{T_{x,9}}{T_{x,5}} \bar{x}_9 \tag{A.21e}$$

$$\bar{x}_6 = c_1 \left(\bar{\xi}_6 - \bar{x}_6\right) T_u \, \bar{u} - \theta_2 \bar{x}_6 \;\; a_{6,5}\theta_4 \frac{T_{x,8}}{T_{x,6}} \bar{x}_8 \;\; a_{6,6}\theta_4 \frac{T_{x,9}}{T_{x,6}} \bar{x}_9 \tag{A.21f}$$

$$\bar{x}_7 = c_1 \left(\bar{\xi}_7 - \bar{x}_7\right) T_u \, \bar{u} - \theta_3 \bar{x}_7 \;\; a_{7,5}\theta_4 \frac{T_{x,8}}{T_{x,7}} \bar{x}_8 \;\; a_{7,6}\theta_4 \frac{T_{x,9}}{T_{x,7}} \bar{x}_9 \tag{A.21g}$$

$$\bar{x}_8 = c_1 \left(\bar{\xi}_8 - \bar{x}_8\right) T_u \, \bar{u} \;\; a_{8,1}\theta_1 \frac{T_{x,5}}{T_{x,8}} \bar{x}_5 \;\; a_{8,2}\theta_2 \frac{T_{x,6}}{T_{x,8}} \bar{x}_6 \;\; a_{8,3}\theta_3 \frac{T_{x,7}}{T_{x,8}} \bar{x}_7 - \theta_4 \bar{x}_8 \tag{A.21h}$$

$$\bar{x}_9 = c_1 \left(\bar{\xi}_9 - \bar{x}_9\right) T_u \, \bar{u} \;\; \theta_5 T_{x,1} \frac{\bar{x}_1 \, \bar{x}_9}{\theta_6 \;\; T_{x,1} \bar{x}_1} \bar{I}_{\mathrm{ac}} - \theta_4 \bar{x}_9 \tag{A.21i}$$

$$\bar{x}_{10} = c_{29} \left(\frac{Tx,1}{T_{x,10}} \bar{x}_1 - \bar{x}_{10} \right) - c_9 \bar{x}_{10} \bar{S}_{\mathrm{H}} \tag{A.21j}$$

$$\bar{x}_{11} = c_{30} \left(\frac{T_{x,3}}{T_{x,11}} \bar{x}_3 - \bar{x}_{11} \right) - c_{10} \bar{x}_{11} \bar{S}_{\mathrm{H}} \tag{A.21k}$$

$$\bar{x}_{12} = c_{31} \left(\frac{T_{x,4}}{T_{x,12}} \bar{x}_4 - \bar{x}_{12} \right) - c_{11} \bar{x}_{12} \bar{S}_{\mathrm{H}} \tag{A.21l}$$

$$\begin{aligned} \bar{x}_{13} = {} & c_{22} T_{x,13}^2 \, \bar{x}_{13}^3 \;\; c_{23} T_{x,13} \, T_{x,14} \, \bar{x}_{13}^2 \bar{x}_{14} \;\; c_{24} T_{x,14}^2 \, \bar{x}_{13} \bar{x}_{14}^2 \;\; c_{25} T_{x,13} \, \bar{x}_{13}^2 \;\; c_{26} T_{x,14} \, \bar{x}_{13} \bar{x}_{14} \\ & c_{12} \frac{T_{x,2}}{T_{x,13}} \, \bar{x}_2 \;\; c_{27} \bar{x}_{13} \end{aligned} \tag{A.21m}$$

$$\begin{aligned} \bar{x}_{14} = {} & c_{24} T_{x,14}^2 \, \bar{x}_{14}^3 \;\; c_{23} T_{x,13} \, T_{x,14} \, \bar{x}_{13} \bar{x}_{14}^2 \;\; c_{22} T_{x,13}^2 \, \bar{x}_{13}^2 \bar{x}_{14} \;\; c_{26} T_{x,14} \, \bar{x}_{14}^2 \;\; c_{25} T_{x,13} \, \bar{x}_{13} \bar{x}_{14} \\ & c_{12} \frac{T_{x,3}}{T_{x,14}} \, \bar{x}_3 - c_{12} \frac{T_{x,11}}{T_{x,14}} \, \bar{x}_{11} \;\; c_{28} \bar{x}_{14} \end{aligned} \tag{A.21n}$$

Therein, $\bar{I}_{\mathrm{ac}}$ and $\bar{S}_{\mathrm{H}}$ are defined as

$$\bar{I}_{\mathrm{ac}} = \frac{c_3}{c_3 \;\; \bar{S}_{\mathrm{H}}^{c_2}} \frac{\bar{x}_4}{\bar{x}_4 \;\; c_8 T_{x,4}} \frac{\theta_7}{\theta_7 \;\; T_{x,12} \, \bar{x}_{12}} \tag{A.22}$$

$$\bar{S}_{\mathrm{H}} = -\frac{\bar{\mathbf{\Phi}}}{2} \;\; \frac{1}{2} \sqrt{\bar{\mathbf{\Phi}}^2 \;\; c_4} \text{ , where} \tag{A.23}$$

$$\bar{\mathbf{\Phi}} = \theta_8 \;\; \frac{T_{x,4} \, \bar{x}_4 - T_{x,12} \, \bar{x}_{12}}{17} - \frac{T_{x,11} \, \bar{x}_{11}}{44} - \frac{T_{x,10} \, \bar{x}_{10}}{60}. \tag{A.24}$$

Normalized measurements:

$$\begin{aligned} \bar{y}_1 = {} & c_{13} \frac{T_{x,13}^2}{T_{y,1}} \, \bar{x}_{13}^2 \;\; c_{14} \frac{T_{x,13} \, T_{x,14}}{T_{y,1}} \, \bar{x}_{13} \bar{x}_{14} \;\; c_{15} \frac{T_{x,14}^2}{T_{y,1}} \, \bar{x}_{14}^2 \;\; c_{16} \frac{T_{x,13}}{T_{y,1}} \, \bar{x}_{13} \\ & c_{17} \frac{T_{x,14}}{T_{y,1}} \, \bar{x}_{14} \;\; \frac{c_{18}}{T_{y,1}} \end{aligned} \tag{A.25a}$$

$$\bar{y}_2 = c_{19} \frac{T_{x,13}}{T_{y,2}} \, \bar{x}_{13} \tag{A.25b}$$

$$\bar{y}_3 = c_{20} \frac{T_{x,14}}{T_{y,3}} \, \bar{x}_{14} \tag{A.25c}$$

$$\bar{y}_4 = -T_{y,4}^{-1} \;\; \log_{10} \bar{S}_{\mathrm{H}} \tag{A.25d}$$

$$\bar{y}_5 = \frac{T_{x,4}}{T_{y,5}} \bar{x}_4 \tag{A.25e}$$

$$\bar{y}_6 = \frac{T_{x,1}}{T_{y,6}} \bar{x}_1 \tag{A.25f}$$

Table 4. *Petersen matrix of ADM1-R3-Core, derived from Weinrich (2017).*

Component i →	1	2	3	4	5	6	7	8	9	
j Process ↓	S_{ac}	S_{ch4}	S_{IC}	S_{IN}	X_{ch}	X_{pr}	X_{li}	X_{bac}	X_{ac}	**Process rate** r_j
1 Fermentation X_{ch}	0.6555	0.0818	0.2245	-0.0169	-1			0.1125		$\theta_1\, x_5$
2 Fermentation X_{pr}	0.9947	0.0696	0.1029	0.1746		-1		0.1349		$\theta_2\, x_6$
3 Fermentation X_{li}	1.7651	0.1913	-0.6472	-0.0244			-1	0.1621		$\theta_3\, x_7$
4 Methanogenesis S_{ac}	-26.5447	6.7367	18.4808	-0.1506					1	$\theta_5\, \frac{x_1}{\theta_6 x_1}\, x_9\, I_{ac}$
5 Decay X_{bac}					0.18	0.77	0.05	-1		$\theta_4\, x_8$
6 Decay X_{ac}					0.18	0.77	0.05		-1	$\theta_4\, x_9$

	2	3	...	...	10	11	12	13	14	
	S_{ch4}	S_{IC}			$S_{\mathrm{ac^-}}$	$S_{\mathrm{hco3^-}}$	S_{nh3}	$S_{\mathrm{ch4,gas}}$	$S_{\mathrm{co2,gas}}$	
7 Dissoziation S_{ac}					-1					$c_{29}\, x_{10} - x_1 \;\; c_9\, x_{10}\, S_{\mathrm{H}}$
8 Dissoziation S_{IC}						-1				$c_{30}\, x_{11} - x_3 \;\; c_{10}\, x_{11}\, S_{\mathrm{H}}$
9 Dissoziation S_{IN}							-1			$c_{31}\, x_{12} - x_4 \;\; c_{11}\, x_{12}\, S_{\mathrm{H}}$
10 Phase transition S_{ch4}	-1							c_{32}		$c_5\, x_2 - c_6\, x_{13}$
11 Phase transition S_{co2}		-1							c_{32}	$c_5\, x_3 - x_{11} - c_7\, x_{14}$